ԵՐԵՎԱՆԻ ՖԻԶԻԿԱՅԻ ԻՆՍՏԻՏՈՒՏ
ЕРЕВАНСКИЙ ФИЗИЧЕСКИЙ ИНСТИТУТ

ЕФИ-467(9)-81

K.V.ALANAKIAN, M.J.AMARIAN, R.A.DEMIRCHIAN,
K.SH.EGIYAN, J.V.KARUMIAN, ZH.L.KOCHAROVA,
M.S.OGANDJANIAN, YU.G.SHARABIAN

SPECTRA OF CUMULATIVE PROTONS IN THE $\gamma + {}^{12}C \to pX$ PROCESS AT γ -QUANTA MAXIMUM ENERGY 4.5 GEV

ԵՐԵՎԱՆ 1981 ЕРЕВАН

ЕФИ-467(9)-81

К.В.АЛАНАКЯН, М.Дж.АМАРЯН, Р.А.ДЕМИРЧЯН,
К.Ш.ЕГИЯН, Дж.В.КАРУМЯН, Ж.Л.КОЧАРОВА,
М.С.ОГАНДЖАНЯН, Ю.Г.ШАРАБЯН

СПЕКТРЫ КУМУЛЯТИВНЫХ ПРОТОНОВ В ПРОЦЕССЕ $\gamma C^{12} \to pX$ ПРИ МАКСИМАЛЬНОЙ ЭНЕРГИИ ТОРМОЗНЫХ γ-КВАНТОВ 4,5 ГЭВ

Приведены экспериментальные энергетические и угловые распределения инклюзивных фотопротонов из ядра C^{12}, облученного тормозными γ-квантами с максимальной энергией 4,5 ГэВ, под угло регистрации в области 20-120° и импульсном интервале 0,4÷1,3 ГэВ/с. Показано, что энергетические распределения фотопротонов в случае кумулятивного образования хорошо описываются экспонентой, тогда как для некумулятивных протонов спектр становится более пологим в области больших энергий. Полученные экспериментальные данные анализируются с точки зрения трех теоретических модельных представлений, пытающихся объяснить образование кумулятивных частиц.

Ереванский физический институт

Ереван 1981

ЕФИ-467(9)-81

K.V.ALANAKIAN, M.J.AMARIAN, R.A.DEMIRCHIAN,
K.SH.EGIYAN, J.V.KARUMIAN, ZH.L.KOCHAROVA,
M.S.OGANDJANIAN, YU.G.SHARABIAN

SPECTRA OF CUMULATIVE PROTONS IN THE $\gamma\,^{12}C \to pX$ PROCESS AT γ-QUANTA MAXIMUM ENERGY 4.5 GEV

Experimental energy and angular distributions of inclusive photoprotons produced on ^{12}C by bremsstrahlung γ-quanta with maximum energy 4.5 GeV, at proton detection angle 20-120^{c} and momenta 0.4 ÷ 1.3 GeV/c are presented. It is shown that in the case of cumulative production the energy distributions of photoprotons are described well by the exponential, whereas for non-cumulative protons the spectrum is flattened out in the high-energy region. The experimental data obtained are analysed from the viewpoint of three theoretical model representations trying to explain the cumulative production of the particles on nuclei.

Yerevan Physics Institute
Yerevan 1981

ЕФИ-467(9)-81

YEREVAN PHYSICS INSTITUTE

K.V.ALANAKIAN, M.J.AMARIAN, R.A.DEMIRCHIAN,
K.SH.EGIYAN, J.V.KARUMIAN, ZH.L.KOCHAROVA,
M.S.OGANDJANIAN, YU.G.SHARABIAN

SPECTRA OF CUMULATIVE PROTONS IN THE $\gamma C^{12} \rightarrow pX$ PROCESS AT γ -QUANTA MAXIMUM ENERGY 4.5 GEV

Yerevan 1981

© Ереванский физический институт, 1981

1. Introduction

According to the cumulative effect [1,2] and nuclear scaling [3,4] the invariant normalized cross section of cumulative baryon production on nuclei by hadrons can be presented in the form

$$\rho = \frac{f}{\sigma_t} = \frac{1}{\sigma_t} E \frac{d^3\sigma}{d^3 p} = C e^{-T/T_0} \simeq C e^{-\beta p^2} \qquad (1)$$

where C, T_0 and B are the representation parameters, σ_t is the total cross section of hadron-nucleus interaction. Parameters $T_0(B)$ and C do not depend on the sort and energy of the incident particle but depend on the direction angle; parameters $T_0(B)$ do not depend on the target-nucleus. The invariance of the parameters $T_0(B)$ and C under initial energy is asymptotic [5,6].

The validity of the representation (1) and the invariance of the coefficient $T_0(B)$ in the processes of cumulative proton production by primary γ -quanta with the energy up to 4.5 GeV [7,8] (and primary neutrino with the energy > 2 GeV [9,10]) on nuclei is proved only for the momentum range of secondary protons up to 0.8 GeV/c.

According to the available theoretical model representations, the exponential form (1) is predicted unambiguously by the cluster model only [11]. At some physically reasonable as-

sumptions this form of the function can be expected in the low-nucleon correlation (LNC) models [12] , if the proton momenta $P_p < 0.8$ GeV/c and quasi-two-particle scaling model [13], if $P_p \leq 1$ GeV/c. In the fluctuan model [14] the exponential form (1) can be obtained only at rather non-realistic assumptions (at asymptotic values of proton momentum and cumulation order).

Thus, the question whether the exponential form (1) is true or not in the region of secondary photoproton momenta $P \geq 1.0$ GeV/c proves principle.

In the present work the energy and angular spectra of photoprotons produced on ^{12}C irradiated with bremsstrahlung γ -quanta with maximum energy 4.5 GeV, at proton detection angle $20 \div 120^{\circ}$ and momenta $0.7 \leq P_p \leq 1.3$ GeV/c (in addition to the region $0.4 \leq P_p \leq 0.8$ GeV/c investigated in our previous works [8,15]) are presented.

2. Experimental set-up

The experimental data are obtained on the "Deuteron" set-up, the detailed description of which is given in [16]. The set-up is located on the way of the photon beam Γ -3 of Yerevan electron synchrotron. The protons with the momentum interval $0.7 \div 1.3$ Gev/c were identified by a magnetic spectrometer using time-of-flight measurement. The spectrometer allows to measure particle momentum with relative spread $\Delta P/P = \pm 6.5\%$ (for $P_p \geq 1.0$ GeV/c) in the solid angle 1.26 millisterad. Velocities of the detected particles were determined with the

help of the time-of-flight measurement system with relative errors $\Delta\beta/\beta \leq 5\%$. Such measurement of velocity and momentum allowed one to separate well protons from other positive particles (mainly from π^+-mesons) up to momenta 1.4 GeV/c. In Fig. 1 a number of time-of-flight spectra are given at fixed values of the current positive polarity in the spectrometer. As it is seen, at $I = 16$a ($P_p = 1.4$ GeV/c) peaks from π^+-mesons (in Fig. 1 peaks from π^+-mesons are on the right) are so far well pronounced. With the decrease of momentum the peaks from protons broaden due to multiple scattering and energy loss in the spectrometer scintillation counters [16].

Analogous spectra are obtained for the current negative polarity in the magnet, in which the events at the places of P peaks are absent.

As the number of protons the areas under the left-side peaks are taken.

3. Experimental results and discussion

The yields of the reaction

$$\gamma + {}^{12}C \rightarrow P + X \qquad (2)$$

have been measured where X is the residual system. Invariant yields of the reaction (1) were determined by the relation

$$f = E\frac{d^3\sigma}{d^3\vec{P}_p} = \frac{E_p}{P_p^2}\frac{N_p}{\Delta\Omega(\Delta P/P)\cdot P\cdot N_n\cdot N_\gamma}\cdot C \qquad (3)$$

where E_p, P_p, N_p are the total energy, momentum and number of detected secondary particles, respectively; $\Delta\Omega$ and ΔP are

the solid angle and momentum measurement spread; N_n and N_γ are the number of nuclei on the way of the beam in the targets and the number of equivalent γ-quanta; C takes into account the contributions of the nuclear absorption and multiple scattering in the target and detector, pairing in the target by γ-quanta as well as efficiency of particle detection by the spectrometer. The obtained values of invariant yield as a function of kinetic energy (secondary particle momentum) and the proton detection angle are presented in Table 1. Only statistical errors are presented. According to our estimates, the systematic errors do not exceed 20%.

3.1. Energy distributions

In Fig. 2 the proton energy spectra from the present measurements (darkened symbols) are given at various exit angles as well as analogous data from [15] for the momentum region $P_p \leq 0.8$ GeV/c (open symbols). The arrow indicates the cumulativity boundary: all the points above the arrow are non-cumulative, whereas the ones below it are cumulative.

It should be mentioned that though the two data series are obtained with different methods at different times (in two independent experiments virtually), no normalizations for the fitting of data were made in Fig. 2. The observed agreement between the two measurement series testifies to small systematic errors in our measurements.

According to Fig. 2, the cumulative proton spectra have an exponential form in the whole momentum measurement region $0.4 \leq P_p \leq 1.3$ GeV/c. In the previous works [8,15] it was

shown that the exponential form is observed for small angles as well (in non-cumulative region up to $\vartheta_p = 20^0$), but only in the momentum range $0.4 \leq P_p \leq 0.8$ GeV/c. As seen from Fig. 2, at increasing the momenta up to 1.3 GeV/c the spectra are flattened out for small angles ($\vartheta_p = 60^0$, 40^0 and 20^0) and to describe them with one exponential becomes impossible.

In [17] it is shown that the cluster model [11] describes very well the angular and energy spectra of the proton photoproduction we obtained [8].

The spectra calculations were carried out by the relation

$$f = \varphi(A) \cdot \exp\left[-\frac{E_p - V \cdot P_p \cdot \cos\vartheta_p}{T_0(V)}\right] \qquad (4)$$

where V is the critical velocity at which the cluster decay takes place; $T_0(V)$ is the parameter of the exponential (actually the temperature of the decaying system) dependent on V. If we introduce variable $T_K = E_p - V P_p$ then, according to (4), the value

$$f/\varphi(A) = \exp\left(-T_K/T_0(V)\right) \equiv F(T_K) \qquad (5)$$

will be a universal function of T_K.

In Fig. 3 the data from Fig. 2 are given in the representation (5). The value of the critical velocity is taken equal to $V = 0.170$ [17]. If the cluster model were true for all the energy and angle values then all the points should have been on the same line. As it is seen, this occurs for the cumulative protons ($\vartheta_p \geq 90^0$) only. In the region of small angles and high energies the deflection of experimental cross sections from the predictions (5) is significant.

In [18] it is shown that in the two-particle correlation

approximation the LNC model gives a satisfactory explanation of the angular dependences of our data [8].

Calculations were done [18] by the relation

$$f = E\frac{d^3\sigma}{d^3\bar{p}} = \Lambda \cdot Z \cdot \sigma^{\gamma N}(K) \cdot |\psi(K)|^2 (m^2 + K^2)^{1/2} \left(1 - \frac{E_{\bar{p}}\, P_{p\parallel}}{2m}\right)^{-1} \qquad (6)$$

where

$$K = \left[m - (E_p - P_{p\parallel})^2 + P_p^2\right]^{1/2} \left[E_p - P_{p\parallel}\right)(2m - E_p + P_{p\parallel}\right]^{-1/2} \qquad (7)$$

is the nucleon momentum in the correlated nucleon pair system [18]; $P_{p\parallel}$ and E_p are the longitudinal momentum and the total energy of the detected proton; $\psi(K)$ is the wave function of the correlated pair; $\sigma^{\gamma N}(K)$ is the total hadronic cross section of γ-quanta; Λ is the constant characterizing the increase of pairing probability in nuclear matter as compared with the free state i.e. deuteron; Z is the atomic number of target nucleus.

From (6) it follows that the value

$$F(K) \equiv |\psi(K)|^2 = f\left[2m - (E_p - P_{p\parallel})\right] \Big/ 2mZ\Lambda\sigma^{\gamma N}(K)\sqrt{m^2 + K^2} \qquad (8)$$

is the universal function of the variable K. In Fig. 4 the data from Fig. 2 are presented as functions of K. As it is seen, the function $F(K)$ universality is observed in the region $K \leq 1$ GeV only.

At $K > 1$ GeV it seems necessary to consider the contributions of highest order correlations, theoretical aspects of which are not sufficiently developed yet.

In the quasi-two-particle scaling model as a universal variable the minimum momentum K_{min} [13] of nucleon in nucleus

is taken which is necessary to observe the detected proton in the given kinematics. K_{min} is expressed through kinematic variables of the reaction in the following way [19]

$$K_{min} = -|\vec{P}_a - \vec{P}_p| + [(E_a + m'_N - E_p)^2 + m_i^2]^{1/2} \qquad (9)$$

where E_a and P_a are the total energy and the momentum of incident particle; m'_N is the mass of the nucleon in nucleus on which the scattering takes place (with a good accuracy $m'_N = m_N - \varepsilon$ where m_N is the free nucleon mass and ε is its binding energy in nucleus); m_i is the scattered particle mass (non-detected). In the photoproduction case m_i is the mass of the particle produced in the collision of the γ -quantum with the nuclear nucleon (mainly π and ρ^0 -mesons).

In this model the invariant normalized cross section can be expressed through two functions [19]:

$$f = G(S, t, d\sigma/dt) \cdot \varphi(K_{min}) \qquad (10)$$

where $S = S(E_\gamma, \vartheta_p, P_p, m_i)$; $t = t(E_\gamma, \vartheta_p, P_p, m_i)$ are common Mandelstam variables; $d\sigma/dt$ is the differential cross section of the proton photoproduction on free nucleon at the same values of S and t. The universal function $\varphi(K_{min})$ is mainly determined [13] by the momentum distribution of nucleons in nucleus.

It follows from (10) that the experimentally determined function

$$\varphi_{ex}(K_{min}) = f_{ex} / G(S, t, d\sigma/dt) \qquad (11)$$

in its explicit form does not depend on the angle and momentum

of detected particles and primary photon energy but is a universal function of K_{min} only.

In the case of primary monochromatic beam and only one possible channel of scattering, as in Frankel experiments, the determination of K_{min} by (9) is single-valued. In our case, first, the primary γ -quanta are of bremsstrahlung character, hence all photons in the energy interval from $E_\gamma = E_{\gamma min}$ to $E_{\gamma max} = 4.5$ GeV contribute to the reaction (2) yield; second, two main channels of scattering (production of π and ρ^0-mesons) contribute. Hence the determination of K_{min} is complicated. Indeed, the calculations show [20] that K_{min} increases with the decrease of γ -quanta energy and increase of scattered particle mass. To illustrate this in Fig. 5 a number of dependences of K_{min} on E_γ for the photoproduction of π (Fig. 5a) and ρ^0 (Fig. 5b) mesons are presented. As it is seen, for the given photoproduction channel K_{min} considerably varies (especially at high energies and small angles of secondary protons) in the interval of E_γ variation from 1 to 4.5 GeV. That is why it makes sense to use instead of K_{min} only its effective value K_{min}^{eff} .

The effective value K_{min}^{eff} can be determined through analogous values for separate channels of K_{min}^{i} in the following way

$$K_{min}^{eff} = \sum_{i=\pi,\rho^0} \alpha_i \, K_{min}^{i} \qquad (12)$$

where α_i is the weight of the scattering channel determined by partial differential cross sections [21] .

As K_{min}^{i} the asymptotic values of K_{min} in Fig. 5 were

taken. It is justified by the fact that, as mentioned in [13], $\varphi(K_{min})$ is a strong exponentially decreasing function of K_{min}, i.e. the main contribution into $\varphi(K_{min})$ give the smallest values of K_{min}.

The final expression for the universal function will have the form

$$\varphi_{exp}(K_{min}^{eff}) = f_{exp} \Big/ \sum_{i=\pi,p} \int_{E_\gamma} G(\beta_i t_i, d\sigma/dt_i)\, dE_\gamma \qquad (13)$$

In Fig. 6 the data from Fig. 2 are presented in representation (13). As it is seen, the experimental points (for $K_{min}^{eff} > 0$) locate mainly nearby one curve. In the region $K_{min}^{eff} \geq 0.5$ this curve is well approximated by $exp(-K_{min}^{eff}/K_0)$ with $K_0 = 0.13$ which is in agreement with the value $K_0 = 0.08 \div 0.14$ from the Frankel hadronic experiments [13].

It should be noted that the observed spreads of a few points (mainly at large momenta and at small angles of detected protons) can be the result of the fact that as K_{min}^{i} the asymptotic values of K_{min} were taken from Fig. 5.

3.2. Angular distributions

In Fig. 7 angular distributions for various kinetic energies of protons are presented. The darkened symbols are from our previous work [15] for $P_p \leq 0.8$ GeV/c, and the open symbols are the new data for $P_p > 0.7$ GeV/c. To make it obvious lines are drawn through the experimental points. The arrows indicate the cumulativity boundaries. Statistic error does not exceed the symbol size.

According to Fig. 7, the angular distributions, first, have a forward directed character [15] which intensifies with the proton energy rise; second, have no peculiarities at the transition boundary between the two kinematic regions.

The angular distributions obtained can be compared with the predictions of the three theoretical models mentioned above (see sec. 3.1). The results of these comparisons are given in Fig. 8a (cluster model), Fig. 8b (LNC model) and Fig.8c (quasi-two-particle scaling model). In all the figures the dashed lines are drawn through experimental points for one energy of protons, and solid lines represent the corresponding calculation curves. The experimental points and the calculation curves are normalized at one point only ($\vartheta_p = 100^0$, $T_p = 80$ MeV). By one and the same figures the corresponding theoretical and experimental distributions are denoted.

According to Fig. 8a, for the proton low energies a good agreement is observed between the experimental and theoretical results as to the cluster model. At increasing the energy of protons this agreement sharply worsens.

In the case of LNC model there is a rather good agreement at low energies and large angles. At increasing the secondary proton energy a notable difference of the form of experimental and calculated angular distributions is observed, and this disagreement is not likely to be eliminated by taking into account the contributions of higher order correlations.

The comparison for the quasi-two-particle scaling model presented in Fig. 8c shaws that for all proton energies not a bad agreement is observed at the angles $\vartheta_p > 80^0$ only. In

the region $\vartheta_p < 80^\circ$ there are strong discrepancies.

It should be noted that for all the three models, besides the normalization constant, there are free parameters which change the form of the calculated angular distributions. For all the models quite a number of calculations have been carried out for various values of these parameters, and in Fig. 8a,b,c the most optimal curves are presented. As to the normalization, it should be emphasized that for the LNC model the normalization constant is about 2-3, for the quasi-two-particle scaling model the minimum value of the normalization constant is some 20-30, and the cluster model does not allow to estimate its value. Thus, as to absolute yields, the closest and most reasonable are the predictions of the LNC model.

In conclusion the authors thank A.Ts.Amatuni for his interest in the work, S.G.Matinyan for constant support, E.M.Laziev and the whole stuff of Yerevan electron synchrotron for providing us with γ -quantum beam.

Table

Invariant yield of protons in the reaction $\gamma\,{}^{12}C \rightarrow pX$ at $E_{\gamma_{max}} = 4.5$ GeV [microbarn GeV^{-2} c^3 ster.$^{-1}$ (equ. γ -quantum)$^{-1}$]

T_p, GeV \ ϑ_p	20°	40°	60°	90°	120°
0.223	4940 ± 130	2820 ± 60	1320 ± 30	408 ± 13	155 ± 4
0.317	2650 ± 70	1110 ± 30	389 ± 10	67.0 ± 3.0	18.6 ± 0.7
0.425	1340 ± 40	444 ± 14	108 ± 3	11.4 ± 0.6	1.66 ± 0.17
0.530	794 ± 23	222 ± 7	33.8 ± 1.4	1.36 ± 0.28	0.178 ± 0.028
0.62	483 ± 14	93.7 ± 3.0	11.2 ± 0.6	0.247 ± 0.051	-

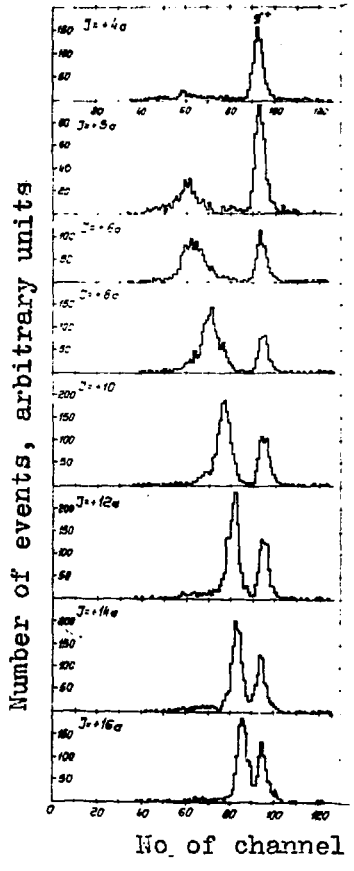

Fig. 1

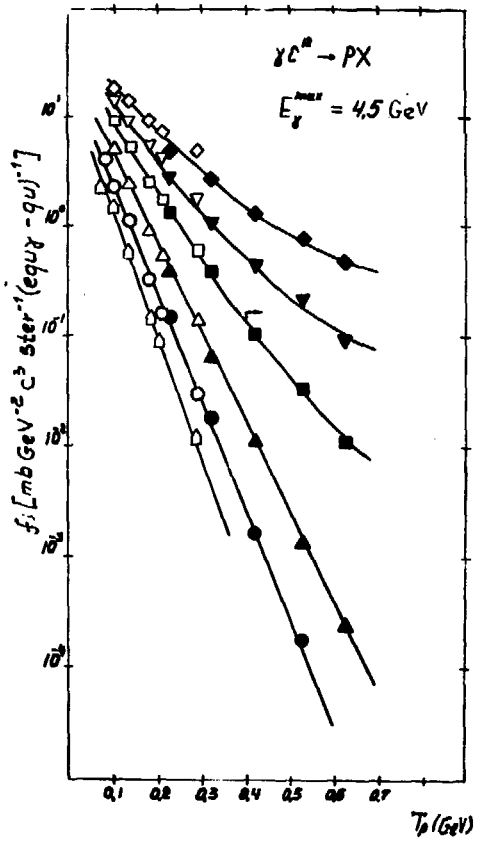

Fig. 2

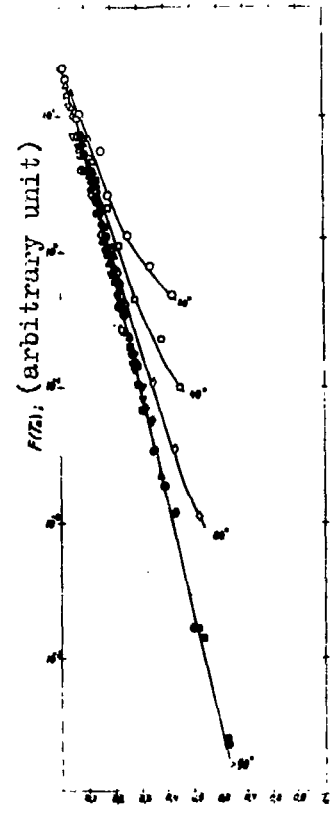

Fig. 3

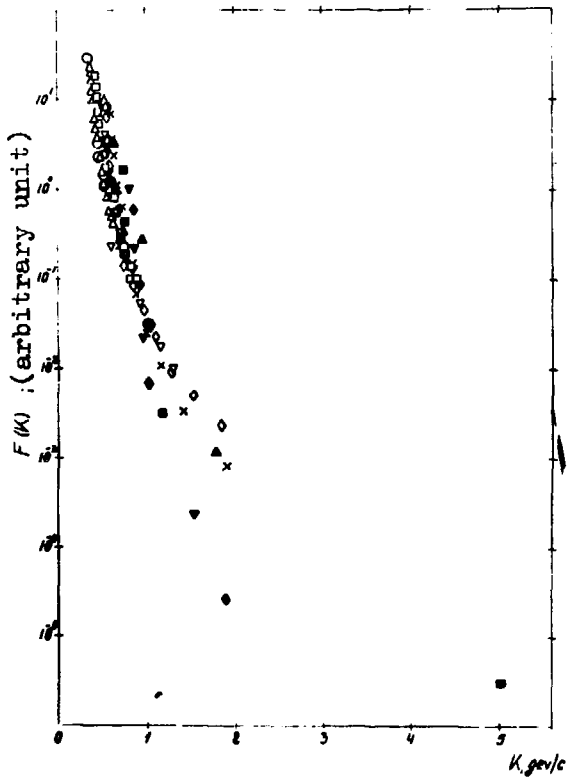

Fig. 4

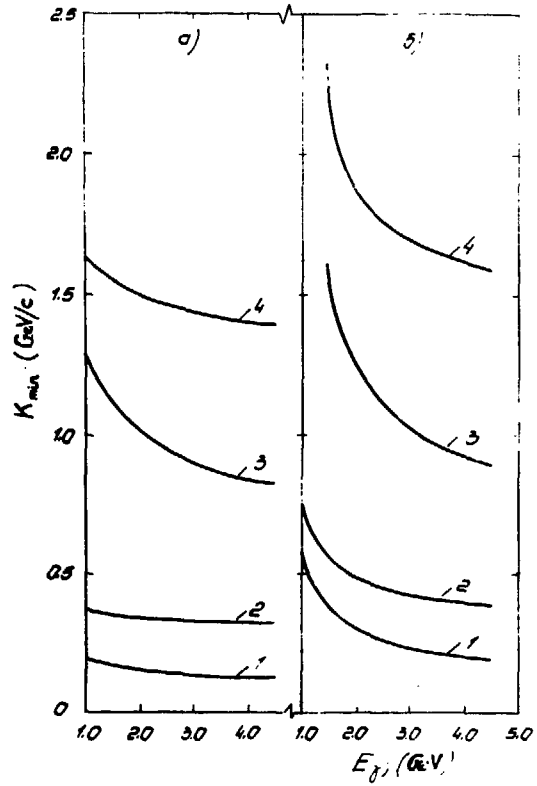

Fig. 5

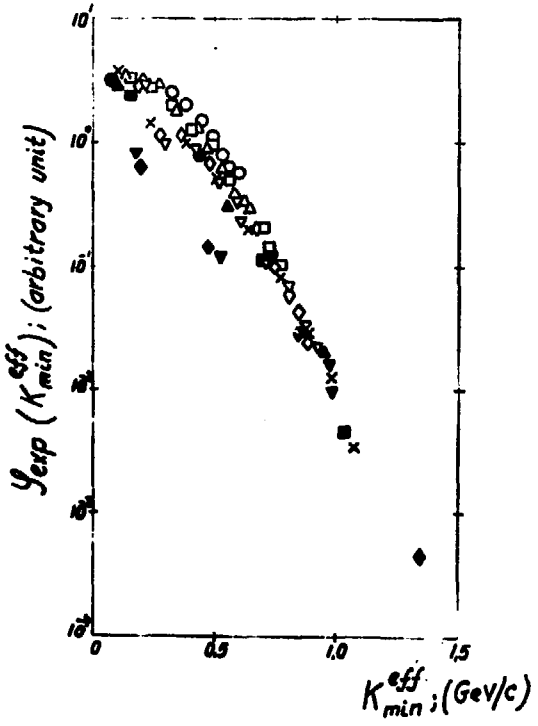
$y_{exp}(K_{min}^{eff})$: (arbitrary unit)
K_{min}^{eff}: (Gev/c)
0
0.5
1.0
1.5

Fig. 6

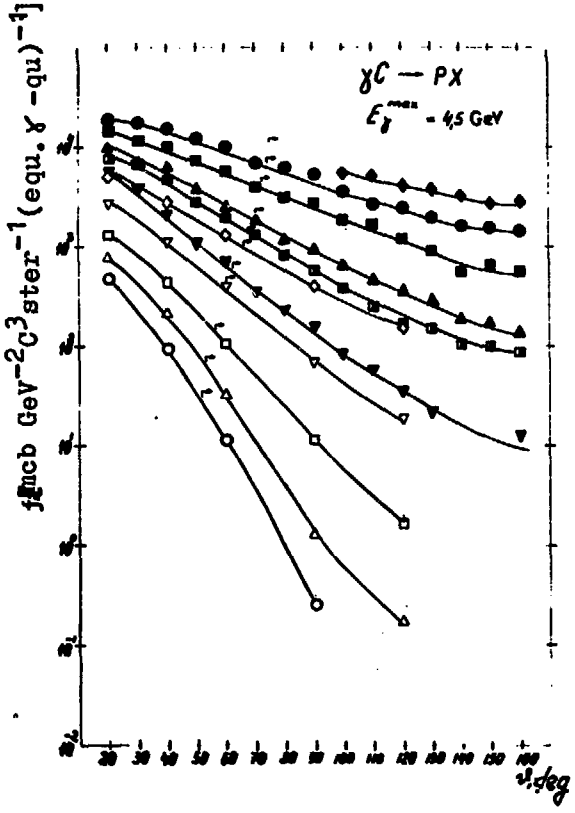
γC — PX
E_γ^{max} = 4,5 GeV
ϑ, deg

Fig. 7

XC→PX
(√s_NN=45 GeV
E d³σ/dp³ [mb GeV⁻² c³ ster⁻¹ (equ. 7 -qu)⁻¹]

Fig. 8 a

XC→PX
(√s_NN=45 GeV
E d³σ/dp³ [mb GeV⁻² c³ ster⁻¹ (equ. 7 -qu)⁻¹]

Fig. 8 b

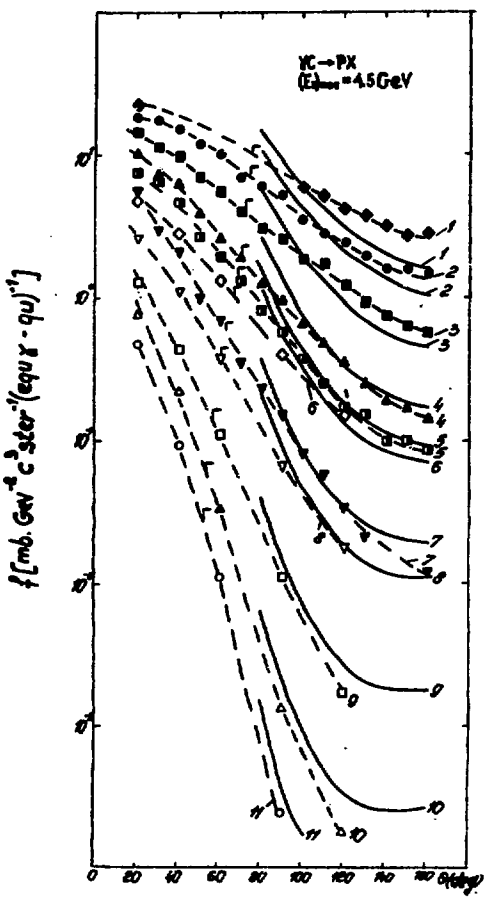
pC→PX
(E)max=4.5GeV
f[mb.GeV⁻²c³ster⁻¹(equ.γ·qu)⁻¹]
0 20 40 60 80 100 120 140 160 180 θ(deg)

Fig. 8 c

FIGURE CAPTIONS

Fig. 1. Mass spectra at current positive polarity in the spectrometer magnet.

Fig. 2. Proton energy spectra of the present measurements (darkened symbols) at $0.7 \leq P_p \leq 1.3$ GeV/c, and analogous data for $P_p \leq 0.8$ GeV/c (open symbols) from the work [15]. ♦, ◊ are for ϑ =20°, ▼, ▽ for 40°, ■, □ for 60°, ▲, △ for 90°, ●, ○ for 120°, ⌂ for 160°.

Fig. 3. Dependence of $F(T_K)$ on T_K (see relation (5)). Experimental points: ○ - for proton detection angle 20°, △ - 30°, □ - 40°, ▽ - 50°, ◊ - 60°, ● - 70°; ▲ - 80°, ■ - 90°, ▼ - 100°, ♦ - 110°, ◑ 120°, ◭ - 130°, ◧ - 140°, ▼ - 150°, ◈ - 160°; at $V = 0.17$ and $T = 52.5$ MeV [17]. The solid lines connect experimental points "by eye".

Fig. 4. Dependence of $F(K)$ on K (see relation (8)). The same symbols as in Fig.2.

Fig. 5. Dependence of K_{min} on E_γ. a - for π -mesons, b - for ρ^0 -mesons. Figures denote: 1. - P_p=0.4 GeV/c; ϑ_p =90°; 2. - P_p=0.4 GeV/c, ϑ_p =120°; 3. - P=1.25 GeV/c, ϑ_p =90°; 4. - P_p=1.25 GeV/c, ϑ_p =120°.

Fig. 6. Dependence of φ_{exp} on K^{eff} (see relation (13)) The same symbols as in Fig. 2.

Fig. 7. Angular dependences of photoprotons of the present measurements (open symbols) at $0.7 \leq P_p \leq 1.3$GeV/d

and analogous data for $P_p \lesssim 0.8$ GeV/c (darkened and semidarkened symbols) [15] ◆ – at proton momentum $P_p = 0.4$ Gev/c, ● – at proton momentum $P_p = 0.44$, ■ – $P_p = 0.52$, ▲ – $P_p = 0.608$, ◨ – $P_p = 0.66$, ◊ – $P_p = 0.69$, ▼ – $P_p = 0.79$, ▽ – $P_p = 0.784$, □ – $P_p = 0.98$, Δ – $P_p = 1.13$, ○ – $P_p = 1.25$ GeV/c. Arrows denote the boundaries between cumulative and non-cumulative regions.

Fig. 8. Comparison of experimental values of angular dependence with calculations on cluster model (a), LNC model (b) and quasi-two-particle scaling model (c). The same symbols as in Fig. 7. Solid lines are those of calculations and dotted lines are drawn through experimental points to make them more obvious. Curves 1 – 11 are numbered for the values of momenta P_p (GeV/c): 1) 0.4, 2) 0.44, 3) 0.52, 4) 0.608, 5) 0.66, 6) 0.69, 7) 0.79, 8) 0.84, 9) 0.98, 10)1.13, 11) 1.25, respectively.

REFERENCES

[1] A.M.Baldin, Kratk. soobsh. po fiz. No 1, 35 (1971); Preprint JINR P7-5769 (1971).

[2] A.M.Baldin et al., Jad. Fiz., 18, 79 (1973); Preprint JINR, P1-5819, (1971).

[3] Yu.D.Bayukov et al., Jad. Fiz., 18, 1246 (1973); Jad.Fiz. 19, 1266 (1974).

[4] G.A.Leksin, Nuclear scaling, XVIII - Int. Conf. High Energy Phys., Tbilisi, 1976; Dubna, 1977, p. A6-3; Prep. ITEP-147 (1976).

[5] A.M.Baldin and V.S.Stavinsky, Proc. of Inetrnational Seminar on High Energy Physics Problems, Dubna 1978, p.261.

[6] A.M.Baldin et al., Jad. Fiz., 21, 1008 (1975); K.Sh.Egiyan, Jad. Fiz., 30, 890 (1979).

[7] K.V.Alanakian et al., Sci. Reports of EPI-173 (19)-76; 174 (20)-76.

[8] K.V.Alanakian et al., Jad. Fiz., 25, 545 (1977); Jad.Fiz. 26, 1018 (1977).

[9] J.P.Berge et al., Phys. Rev. D, 18, 1367 (1978). FERMILAB-PUB-78/55, EXP (1978).

[10] A.A.Ivanilov et al., Pisma v Zh.Eksp. i Teor.Fiz., 30, 390 (1979).

[11] M.I.Gorenstein et al., Jad.Fiz., 26, 788 (1977).

[12] M.I.Strikman and L.L.Frankfurt, Proc. of XII Winter School of LINR, 1977, p.132; Proc. of XIII Winter School of LINR, 1978, p.139.

[13] S.Frankel, Phys. Rev. Lett., 38, 1338, 1977; A.A.Amadc and R.M.Woloshin, Phys. Rev. C 16, 1255 (1977); Phys. Lett. 67B, 46 (1977).

[14] V.V.Burov et al., Preprint JINR, P2-10927 (1977).

[15] K.V.Alanakian et al., Sci. Reports of EPI-220(12)-77.

[16] K.V.Alanakian et al., Sci. Reports of EPI-408(15)-80.

[17] I.G.Bogatskaya et al., Jad.Fiz., 27, 856 (1978).

[18] M.I.Strikman and L.L.Frankfurt, Jad.Fiz., 29, 490(1979).

[19] S.Frankel, Phys. Rev. C 17, 694 (1978).

[20] K.Sh.Egiyan, Proc. of Int. Seminar on High Energy Physics Problems, Dubna, 1978, p.430.

[21] Compilation of Photoproduction Data Above 1.2 GeV P.Joos, DESY-HERA, 70-2, 1970.

The manuscript was received 4 February 1981

К.В.АЛАПАКЯН, М.Дж.АМАРЯН, Р.А.ДЕМИРЧЯН, К.Ш.ЕГИЯН,
Дж.В.КАРУМЯН, Ж.Л.КОЧАРОВА, М.С.ОГАНДЖАНЯН, Ю.Г.ШАРАБЯН

СПЕКТРЫ КУМУЛЯТИВНЫХ ПРОТОНОВ В ПРОЦЕССЕ $\gamma C^{12} \to pX$ ПРИ МАКСИМАЛЬНОЙ ЭНЕРГИИ ТОРМОЗНЫХ γ -КВАНТОВ 4,5 ГЭВ

(на английском языке)

Ереванский физический институт

Тех.редактор А.С.Абрамян

Заказ 326 ВФ-06663 Тираж 299

Препринт ЕФИ Формат издания 60x84/16

Подписано к печати II/У-81г. I,2уч.изд.л. Ц. 9 к.

Издано Отделом научно-технической информации
Ереванский физический институт, Ереван-36, пер.Маркаряна 2

индекс 3624